MCB
Journals.ASM.org

Role of Wnt5a-Ror2 Signaling in Morphogenesis of the Metanephric Mesenchyme during Ureteric Budding

Michiru Nishita,[a] Sen Qiao,[a] Mari Miyamoto,[a] Yuka Okinaka,[a] Makiko Yamada,[b] Ryuju Hashimoto,[c] Kazumoto Iijima,[d] Hiroki Otani,[b] Christine Hartmann,[e] Ryuichi Nishinakamura,[f] Yasuhiro Minami[a]

Department of Physiology and Cell Biology[a] and Department of Pediatrics,[d] Graduate School of Medicine, Kobe University, Kobe, Japan; Department of Developmental Biology[b] and Department of Clinical Nursing,[c] Faculty of Medicine, Shimane University, Izumo, Japan; Department of Bone and Skeletal Research, Institute of Experimental Musculoskeletal Medicine (IEMM), University Hospital Münster, Münster, Germany[e]; Department of Kidney Development, Institute of Molecular Embryology and Genetics, Kumamoto University, Kumamoto, Japan[f]

Development of the metanephric kidney begins with the induction of a single ureteric bud (UB) on the caudal Wolffian duct (WD) in response to GDNF (glial cell line-derived neurotrophic factor) produced by the adjacent metanephric mesenchyme (MM). Mutual interaction between the UB and MM maintains expression of GDNF in the MM, thereby supporting further outgrowth and branching morphogenesis of the UB, while the MM also grows and aggregates around the branched tips of the UB. Ror2, a member of the Ror family of receptor tyrosine kinases, has been shown to act as a receptor for Wnt5a to mediate noncanonical Wnt signaling. We show that Ror2 is predominantly expressed in the MM during UB induction and that *Ror2*- and *Wnt5a*-deficient mice exhibit duplicated ureters and kidneys due to ectopic UB induction. During initial UB formation, these mutant embryos show dysregulated positioning of the MM, resulting in spatiotemporally aberrant interaction between the MM and WD, which provides the WD with inappropriate GDNF signaling. Furthermore, the numbers of proliferating cells in the mutant MM are markedly reduced compared to the wild-type MM. These results indicate an important role of Wnt5a-Ror2 signaling in morphogenesis of the MM to ensure proper epithelial tubular formation of the UB required for kidney development.

Ror2 is a member of the Ror family of receptor tyrosine kinases and acts as a receptor or coreceptor for Wnt5a to activate a noncanonical Wnt signaling pathway and to inhibit the canonical Wnt signaling pathway (1–4). Wnt5a-Ror2 signaling primarily regulates cell polarity and migration in a variety of cell types (1, 5–11). Wnt5a-Ror2 signaling also plays a crucial role in maintaining neural progenitor cells in a proliferative, undifferentiated state in the developing neocortex (12). During mouse development, *Ror2* and *Wnt5a* are expressed in various tissues and organs in spatiotemporally similar manners (13–15). Furthermore, *Ror2*- and *Wnt5a*-deficient mice exhibit overall similarities in their phenotypes (1, 15–18). In humans, mutations within the *Ror2* gene cause an autosomal-recessive form of Robinow syndrome (RRS), which is characterized by short stature, mesomelic limb shortening, brachydactyly, vertebral abnormalities, and a typical fetal face (19, 20). Importantly, several renal abnormalities, including double ureters and kidneys, hydronephrosis, and rudimentary kidney, have been reported to be associated with RRS (21, 22). However, the role of Wnt5a-Ror2 signaling in kidney development is largely unknown.

Development of the metanephric kidney depends on proper interactions between the ureteric epithelium and metanephric mesenchyme (MM) (23). In mice, it begins at embryonic day 10.5 (E10.5) to E11.0, when a single ureteric bud (UB) emerges from the caudal Wolffian duct (WD) and invades the dorsally localized MM. The UB then grows and undergoes branching morphogenesis to form the collecting duct system, while the MM aggregates around the branched tips of the UB and undergoes mesenchymal-epithelial transition and tubulogenesis to form nephrons. Defects in these early induction events can result in congenital anomalies of the kidney and urinary tract (CAKUT), a major cause of renal failure in children (24). Although mutations within several genes have been identified as the cause of human CAKUT, little is known about the molecular pathogenesis of these disorders (25). Accumulating evidence demonstrates that GDNF (glial cell line-derived neurotrophic factor), a growth factor that is produced by the MM, plays central roles in UB induction, acting via its receptor, Ret, expressed in the WD (26–31). Several mechanisms have been reported to regulate GDNF-Ret signaling during UB formation: the transcription factor FoxC1 and Slit2/Robo2 signaling repress the rostral expression of *Gdnf* (32, 33), while Sprouty1, an intracellular inhibitor of receptor tyrosine kinase signaling, reduces the sensitivity of the WD to GDNF (34). Aberrant regulation of GDNF-Ret signaling might result in ectopic activation of GDNF-Ret signaling, leading to ectopic formation of the UBs in the rostral WD.

Here, we show that Ror2 is mainly expressed in the MM during the initiation of UB formation and that both *Ror2*- and *Wnt5a*-deficient embryos exhibit ectopic UBs, resulting in the formation of duplicated ureters and kidneys. Furthermore, loss of *Ror2* or *Wnt5a* causes spatiotemporally aberrant interaction between the MM and WD due to abnormal positioning of the MM, thereby providing the WD with inappropriate GDNF signaling. These re-

Received 10 April 2014 **Returned for modification** 8 May 2014
Accepted 28 May 2014
Published ahead of print 2 June 2014
Address correspondence to Michiru Nishita, nishita@med.kobe-u.ac.jp, or Yasuhiro Minami, minami@kobe-u.ac.jp.
M.N. and S.Q. contributed equally to this work.
Supplemental material for this article may be found at http://dx.doi.org/10.1128/MCB.00491-14.

doi:10.1128/MCB.00491-14

sults suggest that Wnt5a-Ror2 signaling regulates morphogenesis of the MM, an important process ensuring proper epithelial tubular formation of the UB required for kidney development.

MATERIALS AND METHODS

Animals. ICR (Jcl:ICR; CLEA, Japan) mouse embryos were used for expression analysis of Ror2 and Wnt5a. The generation of *Ror2*-deficient mice has been described previously (18). *Wnt5a*-deficient mice were obtained from A. McMahon (15). *HoxB7-EGFP* transgenic mice, which were generated by F. Costantini (35), were obtained from the Jackson Laboratory. All animal experiments in this study were approved by the Institutional Animal Care and Use Committee (permission number P110901-R3) and carried out at the Institute for Experimental Animals, Kobe University Graduate School of Medicine, according to the Kobe University Animal Experimentation Regulations.

Organ culture. Kidney primordia isolated from *HoxB7-EGFP*-expressing embryos at E11.0 or E11.5 were placed on transwell filters (0.4 μm [in diameter] pore size; Corning) and cultured in Dulbecco's modified Eagle's medium (DMEM)–F-12 medium (Sigma) supplemented with 10% (vol/vol) fetal bovine serum and 0.5% (wt/vol) penicillin-streptomycin (Invitrogen) in a humidified atmosphere at 37°C with 5% CO_2. The culture medium was changed every 24 h.

Histology and immunostaining. Embryos were fixed in 4% (wt/vol) paraformaldehyde (PFA) at 4°C overnight, embedded in paraffin, and sectioned at a thickness of 7 μm. The sections were stained with hematoxylin and eosin using a standard protocol or immunostained with anti-Ror2 antibody (1:200), which was prepared as previously described (36). For preparation of cryosections, fixed embryos were equilibrated with 30% (wt/vol) sucrose, embedded in OCT compound (Sakura Finetek), and frozen. Sections were prepared at a thickness of 10 μm and stained with the respective antibodies and DAPI (4′,6-diamidino-2-phenylindole) (Sigma) or phalloidin (Invitrogen). Cryosections were also used for the terminal deoxynucleotidyltransferase-mediated dUTP-biotin nick end labeling (TUNEL) assay (Click-iT TUNEL Alexa Fluor imaging assay kit; Invitrogen). Whole-mount immunofluorescence staining of the kidneys was performed as previously described (37). The following antibodies were purchased commercially: anti-PH3 (ab10543; abcam; 1:400), anti-phospho-Erk (p-Erk) (4370; Cell Signaling; 1:200), anti-Pax2 (PRB-276P; Covance; 1:500), and antipancytokeratin (C2562; Sigma; 1:200).

Whole-mount *in situ* hybridization. The kidneys were fixed in 4% (wt/vol) PFA at 4°C overnight and treated with 10 μg/ml proteinase K in phosphate-buffered saline (PBS) containing 0.1% (vol/vol) Tween 20 (PBST) for 10 min at room temperature. After postfixation with 4% (wt/vol) PFA containing 0.2% (wt/vol) glutaraldehyde for 20 min at room temperature, the tissues were prehybridized in hybridization solution {50% (vol/vol) formamide, 500 mM NaCl, 0.5% (wt/vol) 3-[(3-cholamidopropyl)-dimethylammonio]-1-propanesulfonate (CHAPS), 0.1% (vol/vol) Tween 20, 100 μg/ml yeast tRNA, 0.5 mg/ml heparin, 10 mM piperazine-*N*,*N*′-bis(2-ethanesulfonic acid) (PIPES; pH 6.0), 1 mM EDTA} and hybridized in hybridization solution containing the probe (2 μg/ml) at 63°C overnight. After washing and RNase treatment, specimens were incubated with alkaline phosphatase-conjugated antidigoxigenin antibody (Roche; 1:2,000), and positive signals were visualized with nitroblue tetrazolium (NBT)–5-bromo-4-chloro-3-indolylphosphate (BCIP) (Roche). The cDNAs for *Hoxd11* and *Robo2* probes were obtained by RT-PCR and subcloned into pBluescript and pCRII, respectively. The cDNAs for *Slit2* and *Foxc1* probes were kind gifts from G. Martin (University of California, San Francisco, CA) and T. Kume (Northwestern University School of Medicine), respectively. Digoxigenin-labeled riboprobes for *Ror2*, *Wnt5a*, *Ret*, *Gdnf*, *Hoxd11*, *Robo2*, *Slit2*, and *Foxc1* were prepared as previously described (14, 38, 39).

Quantitative RT-PCR. For separation of the kidney epithelia and mesenchymes, pooled kidneys isolated from the ICR mouse embryos (E11.5) were treated with pancreatin-trypsin enzyme solution (2.5% [wt/vol] pancreatin; 0.5% [wt/vol] trypsin in Ca^{2+}/Mg^{2+} -free Tyrode's saline), and the epithelia and mesenchymes were separated mechanically. Total RNAs were isolated from the separated tissues by using an RNeasy minikit (Qiagen). For expression analysis of *Gdnf* in mutant kidneys, total RNAs were isolated from the kidneys of each individual embryo (E11.0). Quantitative reverse transcription (RT)-PCR was performed as previously described (40). Relative mRNA levels of the respective genes of interest were determined after normalization by levels of 18S rRNA (*18S*). Forward and reverse primer sets for PCR were as follows: *Wnt5a*, 5′-CAAATAGGCAGCCGAGAGAC-3′ and 5′-CTCTAGCGTCCACGAACTCC-3′; *Ror2*, 5′-TGAACACTTGGGAGTGCCTT-3′ and 5′-CTGCTTTCTGTACAACGTTG-3′; *Gdnf*, 5′-CGCTGACCAGTGACTCCAAT-3′ and 5′-AAACGCACCCCCGATTTTTG-3′; *Ret*, 5′-GGCATTAAAGCAGGCTACGGCA-3′ and 5′-GAGGAATAACTGATTGGGAA-3′; *18S*, 5′-ATGGCCGTTCTTAGTTGGTG-3′ and 5′-CGCTGAGCCAGTCAGTGTAG-3′.

Transmission electron microscopy. Transmission electron microscopy (TEM) was performed as previously described (41). Briefly, the kidneys were dissected from E18.5 embryos and fixed in 2.5% (wt/vol) glutaraldehyde and 2% (wt/vol) PFA solution in 0.1 M phosphate buffer (pH 7.4) (PB). After washing with 0.1 M PB containing 7% (wt/vol) sucrose several times and postfixation with 1% (wt/vol) osmium tetroxide in 0.1 M PB, the tissues were dehydrated in graded series of ethanol and embedded in epoxy resin, which was polymerized at 65°C for 48 h. Ultrathin sections (thickness, 0.1 μm) were performed with a diamond knife on an MT-7000 ultramicrotome (RMC Products). Sections were collected onto 40-mesh copper grids and contrasted using 4% (wt/vol) uranyl acetate and lead citrate. The sections were examined under TEM (EM-002B; Topcon) at a low magnification (×500) and a high magnification (×2,000).

RESULTS AND DISCUSSION

Ror2 is expressed in the metanephric mesenchyme during the initial phase of ureteric budding. We first examined the Ror2 expression pattern during kidney development by immunohistochemistry. At E10.5, when a UB starts to emerge from the caudal WD, Ror2 was mainly detected in the MM, which is recognized as a mesenchymal condensation adjacent to the caudal WD (Fig. 1A). Expression of Ror2 in the MM was also observed prominently at E11.5 to E13.5 (Fig. 1B to D), partially decreased at E14.5 (Fig. 1E), and became undetectable at E15.5 (Fig. 1F). Only minimal Ror2 expression could be detected in WD, the UB, the collecting ducts, and the developing nephron tubules at E10.5 to E14.5 (Fig. 1A to E). Immunofluorescence analysis showed strong Ror2 expression at the MM cell membranes surrounding the UB tips (Fig. 1G). In agreement with the expression pattern of Ror2 protein, *Ror2* mRNA was mainly detected in the MM, as assessed by whole-mount *in situ* hybridization (Fig. 1H). In contrast, *Wnt5a* mRNA was detectable in both the MM and WD/UB epithelia at E11.0 (Fig. 1I). These observations were also confirmed by real-time RT-PCR analysis of kidney epithelia (WD/UB) and the nephrogenic mesenchyme (NM), which contains the MM and mesonephric mesenchyme (MesM), both separated from E11.5 kidneys (see Fig. S1A in the supplemental material). Like *Gdnf*, which is exclusively expressed in the MM (42), *Ror2* was highly expressed in the NM, while *Wnt5a* was detected in both the WD/UB and NM/MM (see Fig. S1B in the supplemental material). These findings suggest that Wnt5a-Ror2 signaling might function primarily in the MM during the initial phase of UB formation.

Loss of *Ror2* or *Wnt5a* results in duplicated ureters due to ectopic formation of the ureteric buds. To study the roles of Wnt5a-Ror2 signaling in kidney development, we examined phenotypic features of the kidneys and urinary tracts from *Ror2* and *Wnt5a* knockout (KO) mouse embryos. At E18.5, 54% of the

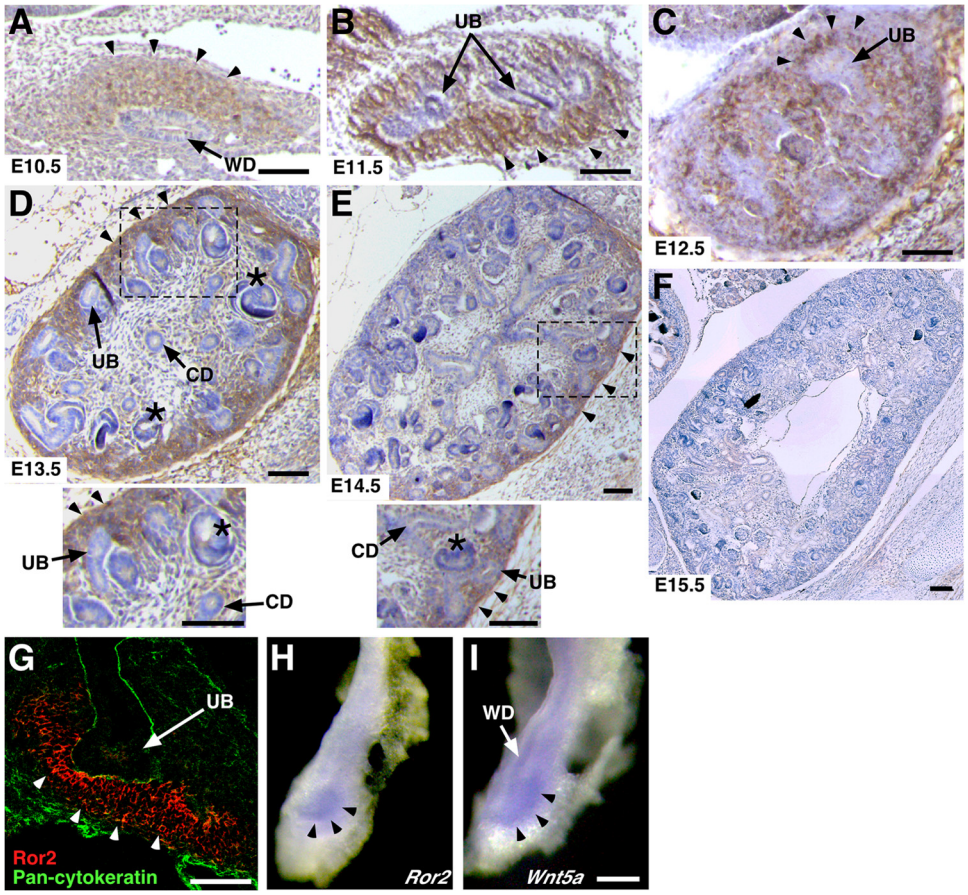

FIG 1 Ror2 is predominantly expressed in the MM during the initial phase of UB formation. (A to F) Immunohistochemical analysis of Ror2 in embryonic kidneys, showing strong Ror2 expression in the MM (arrowheads). The asterisks indicate the developing nephrons. Enlarged images of the boxed regions in panels D and E are shown at the bottom. (G) Double immunofluorescence staining of kidneys (E11.5) with anti-Ror2 (red) and antipancytokeratin (green) antibodies, showing Ror2 expression in the MM (arrowheads) surrounding the tips of the UB (arrow). (H and I) Whole-mount *in situ* hybridization of kidneys (E11.0) with *Ror2* (H) and *Wnt5a* (I) antisense probes. Scale bars, 0.1 mm. CD, collecting duct.

Ror2$^{-/-}$ ($n = 35$) and all of the *Wnt5a*$^{-/-}$ ($n = 6$) embryos examined displayed a duplicated ureter/kidney phenotype either unilaterally or bilaterally, while *Ror2*$^{+/+}$ ($n = 5$), *Ror2*$^{+/-}$ ($n = 18$), *Wnt5a*$^{+/+}$ ($n = 7$), and *Wnt5a*$^{+/-}$ ($n = 12$) embryos had apparently unaffected kidneys (Fig. 2A to F; see Fig. S2A in the supplemental material). In addition, among six *Wnt5a*$^{-/-}$ embryos with duplicated ureters, five embryos exhibited hydronephrosis and hydroureter (Fig. 2C and F), phenotypes that are often caused by impaired connection of the ureter to the bladder and frequently associated with ureter duplication (32–34, 43–45). In contrast, hydroureter was observed in only 9% (3/35) of *Ror2*$^{-/-}$ embryos (see Fig. S2B in the supplemental material). Examination by transmission electron microscopy revealed that most of the renal corpuscles (8/10) in *Wnt5a*$^{-/-}$ kidneys with severe hydronephrosis did not contain capillaries but were occupied by undifferentiated cells. Such abnormalities in the renal corpuscles were somewhat less prominent in *Wnt5a*$^{-/-}$ kidneys without severe hydronephrosis (5/10), and all of the renal corpuscles examined contained normally differentiated cells in wild-type (WT) ($n = 15$) and *Ror2*$^{-/-}$ kidneys ($n = 15$), which did not show any apparent hydronephrosis (see Fig. S3 in the supplemental material). Thus, there is a possibility that abnormal development of the renal corpuscles is associated with hydronephrosis, as suggested by others (46–48). Further studies are required to clarify the mechanisms underlying abnormal development of the renal corpuscles in *Wnt5a* mutants. Our findings indicate that, as in other tissues, such as the limb bud, loss of *Wnt5a* results in more severe defects than loss of *Ror2* in the developing kidney, probably reflecting a redundant function(s) of another Ror family member, Ror1, which is also expressed in the urogenital tract (13). Importantly, several renal abnormalities, including double ureters/kidneys and hydronephrosis, are associated with an autosomal-recessive form of RRS (21, 22), which is caused by mutations within *Ror2* (19, 20), indicating that *Ror2*$^{-/-}$ and *Wnt5a*$^{-/-}$ mice can serve as a model for understanding the pathogenic mechanisms of renal malformations in individuals with RRS. Interestingly, the phenotypes observed in *Ror2*$^{-/-}$ and *Wnt5a*$^{-/-}$ kidneys are characteristic of human CAKUT, which is caused primarily by abnormalities during the initial phases of kidney induction (24), suggesting that impaired Wnt5a-Ror2 signaling may potentially be involved in the pathogenesis of CAKUT in humans.

Since formation of duplex ureters and kidneys is attributable to ectopic formation of the UB (33, 43), we next examined UB formation in *Ror2* KO and *Wnt5a* KO embryos. To this end, these mutant mice were crossed with *HoxB7-EGFP* mice, which express enhanced green fluorescent protein (EGFP) in the WD and its

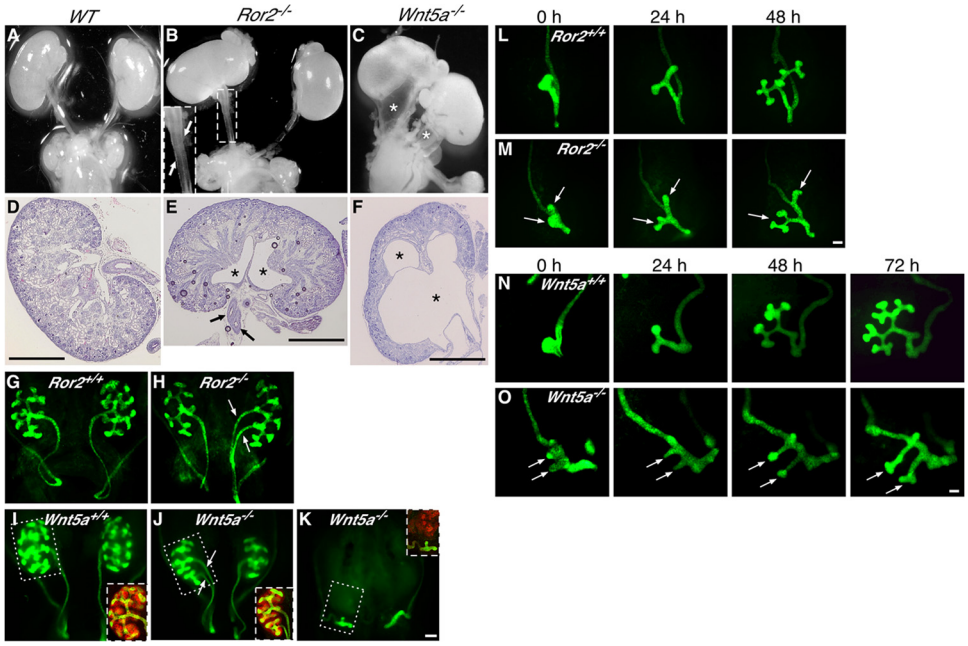

FIG 2 Abnormal kidney development in *Ror2*- and *Wnt5a*-deficient mice. (A to C) Urogenital systems from WT (A), $Ror2^{-/-}$ (B), and $Wnt5a^{-/-}$ (C) embryos at E18.5. The inset in panel B shows a magnified view of the boxed region with duplicated ureters (arrows). The asterisks in panel C indicate hydroureters. (D to F) Hematoxylin and eosin staining of kidneys (E18.5). The arrows and asterisks indicate duplicated ureters and renal pelves, respectively. Scale bars, 1 mm. (G to K) *HoxB7-EGFP* (green)-expressing kidneys that were isolated from embryos with the indicated genotypes at E12.5. The arrows indicate duplicated UBs. The insets in panels I to K show images of the boxed regions after whole-mount immunofluorescence staining with anti-Pax2 antibody (red). Scale bar, 0.1 mm. (L to O) Organ culture of *Ror2*- and *Wnt5a*-deficient kidneys. *HoxB7-EGFP*-expressing kidneys were isolated from embryos with the indicated genotypes at E11.0 (designated 0 h) and cultured for up to 48 h (L and M) or 72 h (N and O). The arrows indicate duplicated UBs. Scale bars, 0.1 mm.

derivatives, the UB and collecting ducts, and then UB formation was analyzed in whole-mount kidneys at E11.5 to E12.5. We found that 52% of $Ror2^{-/-}$ ($n = 25$) and 42% of $Wnt5a^{-/-}$ ($n = 19$) embryos indeed exhibited duplicated ureters with branched UB tips at E11.5 to E12.5, while all of their $Ror2^{+/+}$ ($n = 21$) and $Wnt5a^{+/+}$ ($n = 15$) littermates had a single ureter (Fig. 2G to J; see Fig. 5A to D). Duplicated ureters are known to arise as a consequence of either the formation of two separate UBs from the WD (complete duplication) or premature branching (bifurcation) of a single UB (incomplete duplication) (49). Among the mutant kidneys with duplicated ureters, 38% ($Ror2^{-/-}$) and 50% ($Wnt5a^{-/-}$) of the kidneys showed complete duplicated ureters while the remainder showed incomplete duplicated ureters. Although these two types of duplication appear to be distinct, their underlying mechanisms may be similar, since both induction of the UB and its initial branching are driven by signals from adjacent MM (23), suggesting an important role of Wnt5a-Ror2 signaling in the properties of the MM. We also found that 53% of $Wnt5a^{-/-}$ embryos ($n = 19$; E11.5 to E12.5) failed to form branched UBs on either side but had one or multiple short UBs or bulges instead (Fig. 2K; see Fig. 5E), a phenotype that was not observed in $Ror2^{-/-}$ embryos, probably due to functional redundancy between Ror1 and Ror2. This finding was unexpected, since we did not observe renal agenesis in $Wnt5a^{-/-}$ embryos at E18.5, raising the possibility that the short, unbranched UB(s) observed at E11.5 to E12.5 could grow and branch to develop the duplicated kidneys and ureters by E18.5 *in vivo*, even though the short, unbranched UB at E11.5 failed to branch within 3 days of organ culture (see Fig. 5E′), probably reflecting the delayed UB outgrowth of the mutant kidneys, as mentioned below.

To examine genetic interactions between *Wnt5a* and *Ror2*, we crossed $Ror2^{+/-}$ $Wnt5a^{+/-}$ mice with $Ror2^{+/-}$ mice and assessed the ureter and kidney phenotypes of the embryos at E12.5. All of the $Ror2^{+/-}$ $Wnt5a^{+/-}$ embryos examined showed a single ureter on either side ($n = 7/7$), while $Ror2^{-/-}$ $Wnt5a^{+/-}$ embryos exhibited unilateral ($n = 3/7$) or bilateral ($n = 1/7$) agenesis of the ureter/kidney or double ureters ($n = 2/7$) (see Fig. S4 in the supplemental material). Among the 3 embryos with unilateral ureter/kidney agenesis, 1 also had duplicated ureters in the contralateral kidney (see Fig. S4 in the supplemental material). Since agenesis of the ureter/kidney was observed in $Wnt5a^{-/-}$ but not $Ror2^{-/-}$ embryos at E12.5 (Fig. 2G to K; see Fig. S4 in the supplemental material), our results indicate that loss of one allele of *Wnt5a* can enhance the ureter/kidney defects in $Ror2^{-/-}$ embryos, resembling those in $Wnt5a^{-/-}$ embryos. The observed genetic interactions between *Wnt5a* and *Ror2* suggest that Wnt5a and Ror2 act in the same pathway during kidney development.

We next analyzed the pattern of UB formation by organ culture of kidney rudiments isolated at E11.0. Explants from WT E11.0 embryos exhibited a single unbranched UB at the caudal WD, which then elongated and branched once to form a T-shaped UB within 24 h of culture and branched further within 48 h (Fig. 2L and N). In contrast, explants from $Ror2^{-/-}$ or $Wnt5a^{-/-}$ littermates exhibited a single or two closely positioned bulges at E11.0 (0 h), which then developed into two distinctly separated UBs within 24 h of culture and grew further to form duplex T-shaped UBs within 48 to 72 h (Fig. 2M and O). The process of UB formation in these mutant kidneys was markedly delayed compared with WT kidneys (Fig. 2L to O). Taken together, these results suggest that Wnt5a-Ror2 signaling might be required for restrict-

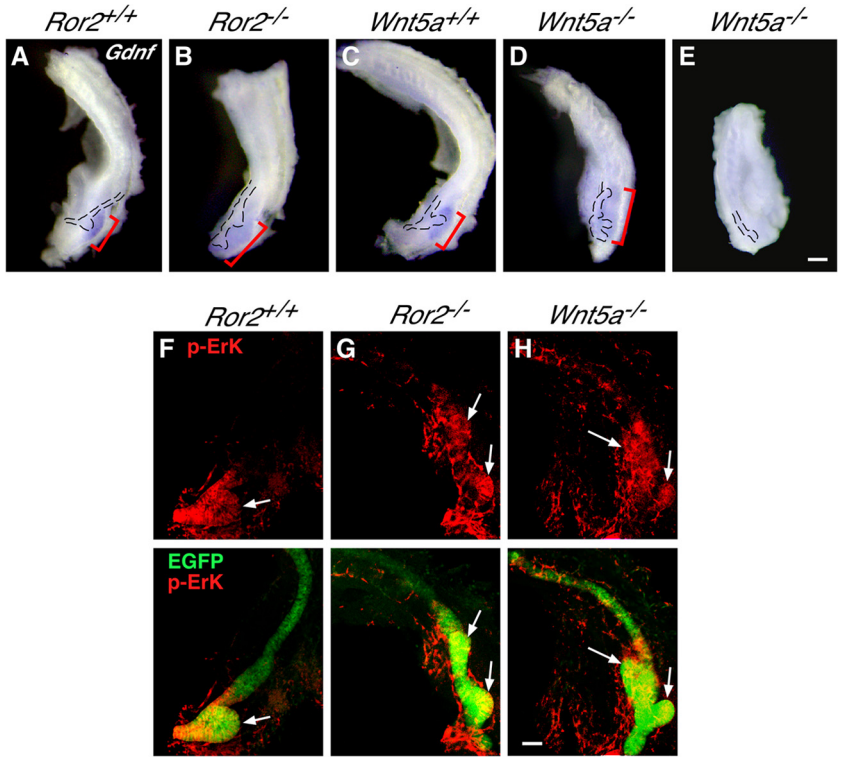

FIG 3 *Gdnf* expression is mislocalized in *Ror2*- and *Wnt5a*-deficient kidneys. (A to E) Whole-mount *in situ* hybridization of kidneys (E11.0) with *Gdnf* antisense probe (brackets). The WD and UBs are outlined. Scale bar, 0.1 mm. (F to H) Whole-mount immunofluorescence staining of kidneys (E11.0) expressing *HoxB7-EGFP* (green) with anti-p-Erk antibody (red). Images of anti-p-Erk staining alone (top row) and merged images (bottom row) are shown. Arrows indicate UBs. Scale bar, 0.1 mm.

ing the budding of the WD to a single site and for proper UB outgrowth and subsequent branching.

***Gdnf* is mislocalized in *Ror2*- and *Wnt5a*-deficient kidneys.** Accumulating evidence demonstrates that GDNF functions as a primary induction factor of the UB by acting through the Ret receptor expressed in the WD (26–31). Since the expression pattern of *Ret* was apparently unaffected in $Ror2^{-/-}$ and $Wnt5a^{-/-}$ kidneys (see Fig. S5 in the supplemental material), we then examined the expression of *Gdnf* in $Ror2^{-/-}$ and $Wnt5a^{-/-}$ kidneys by whole-mount *in situ* hybridization. At E11.0, *Gdnf* expression was highly concentrated around the tip of the single UB in WT kidneys (Fig. 3A and C). Importantly, however, in $Ror2^{-/-}$ and $Wnt5a^{-/-}$ kidneys, *Gdnf* expression was spread rostrally relative to the normal UB, which arises at the caudal end of the WD, but its signal intensity was reduced compared with that detected in WT kidneys (Fig. 3A to D). The rostral spread of the *Gdnf*-expressing region is consistent with the observation that the ectopic UB(s) arose rostrally compared to the normal UB's position (Fig. 3A to D). An essentially identical pattern of *Gdnf* expression was observed in $Ror2^{-/-}$ and $Wnt5a^{-/-}$ kidneys. However, in some $Wnt5a^{-/-}$ kidneys with impaired UB outgrowth, *Gdnf* was not detected (Fig. 3E). Quantitative RT-PCR analysis revealed that expression levels of *Gdnf* in E11.0 kidneys were comparable among different genotypes, except for some $Wnt5a^{-/-}$ embryos, where *Gdnf* was only marginally detected (see Fig. S6 in the supplemental material). Together with the results of *in situ* hybridization, these data indicate that, although *Gdnf* expression is more widespread spatially, its local concentration is reduced in $Ror2^{-/-}$ and $Wnt5a^{-/-}$ kidneys with duplicated UBs, at least at E11.0. Our results also suggest that the reduced local concentration of *Gdnf* may cause the delay of UB outgrowth in $Ror2^{-/-}$ and $Wnt5a^{-/-}$ kidneys. We next examined the activity of Erk signaling, one of the main downstream signaling pathways elicited by GDNF-Ret (50, 51), by whole-mount immunofluorescence staining. We found high levels of p-Erk at the single UB in WT kidneys, as well as the duplicated UBs in $Ror2^{-/-}$ and $Wnt5a^{-/-}$ kidneys (Fig. 3F to H), consistent with the spatial expression pattern of *Gdnf* surrounding the UB(s). Taken together, these results support the notion that loss of Wnt5a-Ror2 signaling results in mislocalization of *Gdnf* expression in the MM, which induces ectopic activation of GDNF-Ret signaling in the WD, leading to ectopic formation of the UB.

Loss of *Ror2* or *Wnt5a* results in malpositioning and growth reduction of the metanephric mesenchyme. It has been reported that loss of *Slit2*, *Robo2*, or *Foxc1* results in ectopic formation of the UBs due to aberrant expression of *Gdnf* (32, 33). Whole-mount *in situ* hybridization of E11.0 kidneys revealed that the expression patterns of these genes are virtually unaffected by loss of either *Ror2* or *Wnt5a* (see Fig. S7 in the supplemental material), suggesting that Wnt5a-Ror2 signaling may regulate spatial expression of *Gdnf* and UB formation through mechanisms independent of signaling mediated by Slit2/Robo2 and Foxc1. It has been well established that mutual interaction between the MM and UB is required for maintaining expression of *Gdnf* in the MM, thereby supporting further outgrowth and branching morphogenesis of the UB (23, 52). Since Ror2 is predominantly expressed in the MM during the initial phase of UB formation, we hypothesized that

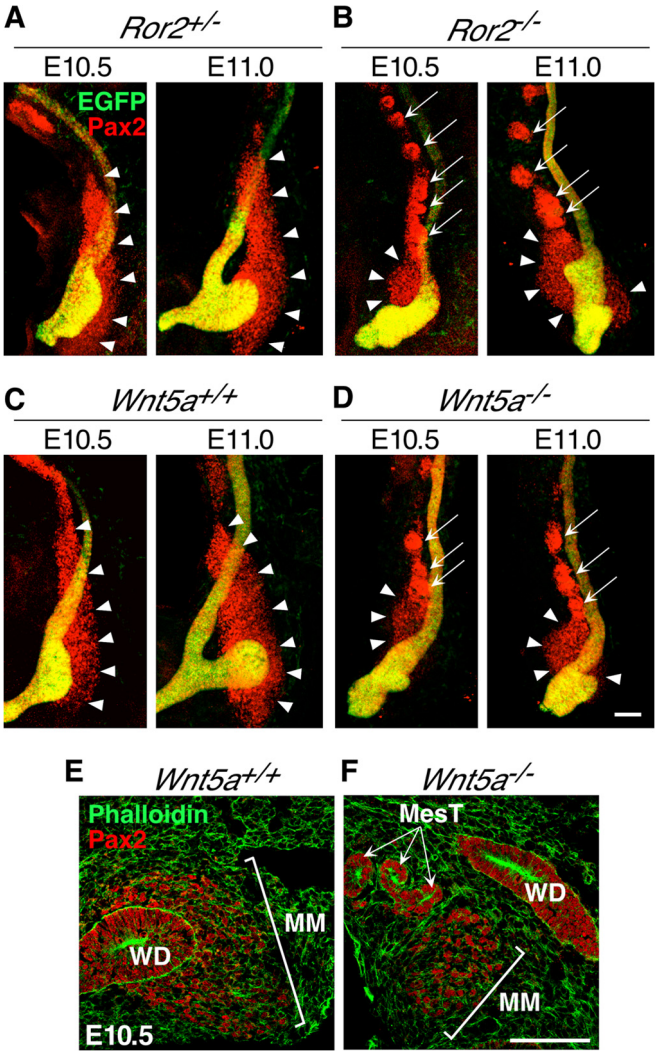

FIG 4 Aberrant morphogenesis of the MM in *Ror2*- and *Wnt5a*-deficient kidneys during UB induction. (A to D) Kidneys expressing *HoxB7-EGFP* (green) were isolated from embryos at E10.5 and E11.0 and subjected to whole-mount immunofluorescence staining with anti-Pax2 antibody (red). All images are lateral views with anterior at the top and dorsal at the right. The arrowheads and arrows indicate the MM and MesTs, respectively. Scale bar, 0.1 mm. (E and F) Frozen sections of kidneys (E10.5) were stained with phalloidin (green) and anti-Pax2 antibody (red). Scale bar, 0.1 mm.

loss of *Ror2* or *Wnt5a* causes aberrant morphogenesis of the MM, which may give rise to inappropriate interaction between the MM and WD, resulting in ectopic budding and mislocalized *Gdnf* expression. To confirm this notion, the mutant kidneys expressing *HoxB7-EGFP* were isolated from embryos at E10.5 and E11.0, and the spatial distribution of the MM was determined by whole-mount immunofluorescence staining with anti-Pax2 antibody, which labels the MesM, WD, and UB, in addition to the MM. As reported previously (37), at E10.5, the MM was located along the caudal WD, almost separated from the MesM, and stretched dorsally but not ventrally at the UB domain in WT and $Ror2^{+/-}$ kidneys (Fig. 4A and C). In accordance with the dorsal positioning of the MM, in WT and $Ror2^{+/-}$ kidneys, the UB was bulged dorsally at E10.5 (Fig. 4A and C). At E11.0, we found a well-developed MM that was clearly separated from the caudal WD and accumulated around the UB tip with concomitant outgrowth of the UB in WT kidneys (Fig. 4A and C). In contrast, the MM in $Ror2^{-/-}$ and $Wnt5a^{-/-}$ kidneys was relatively small and did not stretch to the dorsal side of the WD at E10.5 (Fig. 4B and D). At E11.0, the mutant MM was still mainly positioned at the ventral side and only slightly at the dorsal side of the caudal WD without any intervening space between the MM and WD (Fig. 4B and D). An essentially identical pattern of MM positioning was observed in $Ror2^{-/-}$ and $Wnt5a^{-/-}$ kidneys, consistent with the pattern of their *Gdnf* and pErk distribution. Thus, in addition to the fact that the mutant MM was somewhat smaller, it was abnormally juxtaposed to the caudal WD continuously during initial UB formation, implying the presence of a putative ectopic UB stimulating

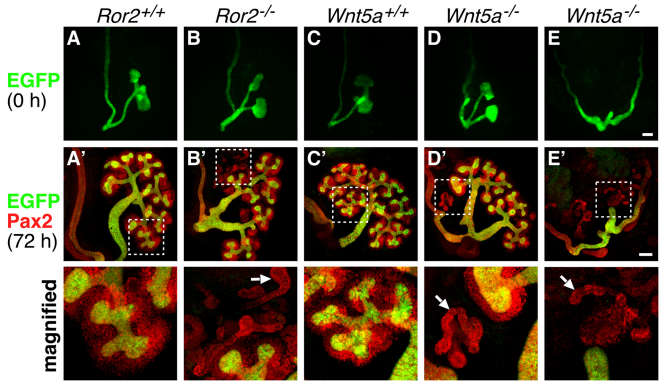

FIG 5 Impaired UB outgrowth in *Wnt5a*-deficient kidneys is associated with the loss of proper interaction between the MM and UB. (A to E) Kidneys expressing *HoxB7-EGFP* (green) were isolated from embryos at E11.5 with the indicated genotypes. (A′ to E′) After organ culture for 72 h, the kidneys were subjected to whole-mount immunofluorescence staining with anti-Pax2 antibody (red). Magnified images of the boxed regions are shown at the bottom. The arrows indicate MesTs. Scale bars, 0.1 mm.

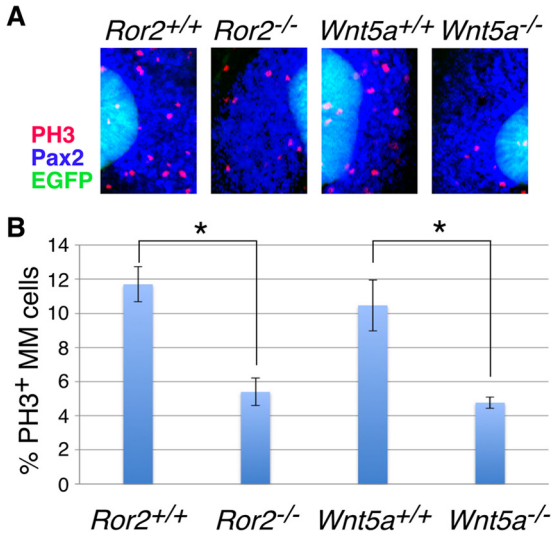

FIG 6 Decreased mitotic cells in the MM of *Ror2*- and *Wnt5a*-deficient kidneys. (A) Kidneys (E11.0) expressing *HoxB7-EGFP* (green) were subjected to whole-mount immunofluorescence staining with anti-Pax2 (blue) and anti-PH3 (red) antibodies. (B) Relative proportions of PH3-positive cells (means ± standard deviations [SD]; $n = 3$) in the MM (Pax2-positive, EGFP-negative cells). More than 300 cells were counted for each sample. *, $P < 0.005$; *t* test.

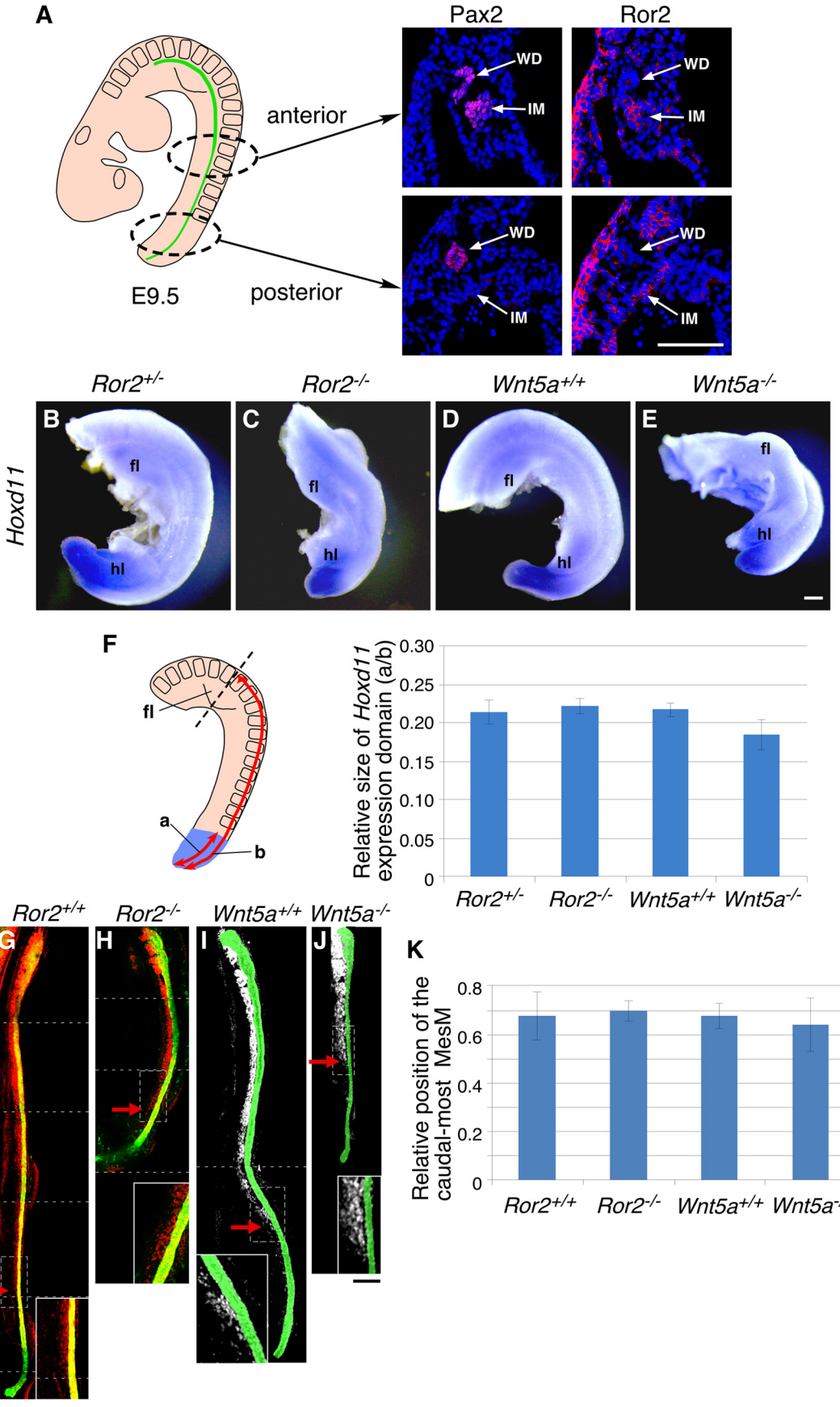
A
Pax2
Ror2
WD
IM
anterior
posterior
E9.5
Ror2+/-
Ror2-/-
Wnt5a+/+
Wnt5a-/-
Hoxd11
B
C
D
E
fl
hl
F
a
b
Relative size of Hoxd11 expression domain (a/b)
0.30
0.25
0.20
0.15
0.10
0.05
0
Ror2+/-
Ror2-/-
Wnt5a+/+
Wnt5a-/-
G
H
I
J
K
Relative position of the caudal-most MesM
0.8
0.6
0.4
0.2
0

factor, like GDNF, in the WD continuously. These results suggest that Wnt5a-Ror2 signaling is required for proper positioning of the MM during initial UB formation.

To further study MM formation in *Ror2*$^{-/-}$ and *Wnt5a*$^{-/-}$ embryos after E11.0, mutant kidneys were isolated at E11.5, when duplication (Fig. 5B and D) or outgrowth defects (Fig. 5E) of the UB were apparent in the mutant embryos. After 72 h of organ culture, MM formation was examined (Fig. 5A′ to E′). As shown, each of the duplex UBs in both *Ror2*$^{-/-}$ and *Wnt5a*$^{-/-}$ kidneys formed numerous UB tips that were surrounded by the MM, as observed in WT kidneys (Fig. 5A′ to D′), indicating that in these mutants with duplicated UBs, MM formation by itself was unaffected. In contrast, *Wnt5a*$^{-/-}$ kidneys with impaired UB outgrowth at E11.5 failed to form a branched UB even after 72 h in culture, and the MM was poorly developed and/or maintained without associating with the UB (Fig. 5E′). Similar results were obtained with *Wnt5a*$^{-/-}$ kidneys isolated from embryos at E12.5 (Fig. 2I to K, insets). These findings indicate that although Wnt5a-Ror2 signaling is required for proper ureteric budding from the WD, once the UB grows to a certain extent, mutual interaction between the UB and MM supports their further outgrowth and branching, irrespective of Wnt5a-Ror2 signaling, by maintaining *Gdnf* expression. *Wnt5a*$^{-/-}$ kidneys with impaired UB outgrowth at E11.5 may fail to create proper interactions between the UB and MM, resulting in arrest of their further growth and UB branching.

Interestingly, we found ectopic formation of mesonephric tubules (MesTs) in close proximity to the MM in *Ror2*$^{-/-}$ and *Wnt5a*$^{-/-}$ kidneys at E10.5 and E11.0 (Fig. 4B and D). Section immunofluorescence analysis confirmed the presence of extratubular MesT structures adjacent to the MM in *Wnt5a*$^{-/-}$ kidneys, while this was never detected in WT kidney sections that contained the MM (Fig. 4E and F). Ectopic formation of MesTs was also observed in the section of *Ror2*$^{-/-}$ kidneys (data not shown), as well as in organ-cultured *Ror2*$^{-/-}$ and *Wnt5a*$^{-/-}$ kidneys with duplicated UBs (Fig. 5B′ and Fig. 5D′). However, induction of the ectopic MesTs was not correlated with the presence of multiple UBs, since it also occurred in *Ror2*$^{-/-}$ and *Wnt5a*$^{-/-}$ kidneys with a single UB (data not shown), as well as in *Wnt5a*$^{-/-}$ kidneys with impaired UB outgrowth and branching (Fig. 5E′). During kidney development, the MesTs are known to arise adjacent to the rostral WD through mesenchymal-epithelial transition (MET) of the rostral MesM (53), where Wnt9b secreted from the WD plays a central role by activating the canonical Wnt pathway (54) while the caudal MesM disappears through apoptosis (37). Since Wnt5a-Ror2 signaling can inhibit the canonical Wnt pathway (2), it is conceivable that loss of *Ror2* or *Wnt5a* might induce ectopic activation of the canonical Wnt pathway, resulting in the formation of extra-MesTs.

We next examined whether the smaller size of the MM in mutant kidneys at E10.5 to E11.0 (Fig. 4A to D) is due to decreased cell proliferation or increased apoptosis. TUNEL staining revealed very few apoptotic cells at comparable levels in both WT and mutant kidneys (data not shown). On the other hand, *Ror2*$^{-/-}$ and *Wnt5a*$^{-/-}$ kidneys showed a statistically significant decrease in phospho-histone H3 (PH3)-positive proliferating cell numbers in the MM adjacent to the UB (Fig. 6), suggesting that a decreased rate of cell proliferation is at least partly responsible for the smaller size of the MM in the mutant kidneys during the initial phase of UB formation.

Loss of *Ror2* or *Wnt5a* does not affect the positioning of the posterior IM that gives rise to the metanephric mesenchyme. It has been shown that at E9.5 the intermediate mesoderm (IM) is differentially patterned along its anterior-posterior axis, i.e., the Pax2-positive anterior IM (MesM), which gives rise to the mesonephros but not the metanephros, and the Pax2-negative, Hox11-positive posterior IM, which contains the precursor of the MM and therefore can develop the metanephros (55). As mentioned above, loss of either *Ror2* or *Wnt5a* causes compromised posterior extension (15, 18), raising the possibility that the aberrant positioning of the MM would be secondary to mispositioning of the posterior IM, which gives rise to the MM. In fact, Ror2 was expressed in the Pax2-negative posterior IM as well as the Pax2-positive anterior IM at E9.5 (Fig. 7A). We examined the expression pattern of the *Hox11* family gene *Hoxd11*, since its expression is known to be restricted to the posterior, metanephric level of the IM at E9.5 and to be essential to specify the metanephric region along the anterior-posterior axis of the IM (53, 56). Whole-mount *in situ* hybridization in E9.5 embryos showed expression of *Hoxd11* in the posterior ends of both control and mutant (*Ror2*$^{-/-}$ and *Wnt5a*$^{-/-}$) embryos in similar patterns (Fig. 7B to E). The sizes of the *Hoxd11*-expressing domain relative to the trunk size along the vertebrae were almost comparable between the control and mutant embryos (Fig. 7F), indicating that the posterior IM was normally patterned and positioned along the anterior-posterior axis at E9.5. In agreement with this result, the proportions of proliferating mesenchymal cells around the posterior WD in E9.5 kidneys were similar in both the control and mutant embryos (data not shown). We next examined the position of the anterior IM, i.e., the MesM, by anti-Pax2 whole-mount immunostaining, since the MesTs, derivatives of the MesM, were aberrantly positioned in the metanephric region of *Ror2*$^{-/-}$ and *Wnt5a*$^{-/-}$ embryos at E10.5 (Fig. 4). Importantly, the relative positions of the caudalmost MesM along the WD were not significantly different between the control and mutant embryos (Fig. 7G to K), indicating that, like the posterior IM, the anterior IM is normally positioned, at least at E9.5. Taken together, these results suggest that the aberrant positioning of the MM in *Ror2* and *Wnt5a* mutants at E10.5 is not due to the mispatterning or mis-

FIG 7 Normal positioning of the posterior IM in *Ror2*- and *Wnt5a*-deficient embryos at E9.5. (A) Immunofluorescence staining of E9.5 embryos with anti-Pax2 (red) (left) and anti-Ror2 (red) (right), counterstained with DAPI (blue). Ror2 is detected in both the anterior and posterior IM. Scale bar, 0.1 mm. (B to E) Whole-mount *in situ* hybridization of embryos (E9.5) with *Hoxd11* antisense probe. fl, forelimb bud; hl, hindlimb bud. Scale bar, 0.1 mm. (F) Length from the tail tip to the rostral limit of the *Hoxd11*-expressing domain (a) relative to the length from the tail tip to the level of the midforelimb bud along the vertebrae (b) (means ± SD; $n = 3$). (G to J) Kidney rudiments were isolated from *Ror2*$^{+/+}$ and *Ror2*$^{-/-}$ embryos expressing *HoxB7-EGFP* (G and H, green) or *Wnt5a*$^{+/+}$ and *Wnt5a*$^{-/-}$ embryos (I and J) at E9.5 and subjected to whole-mount immunofluorescence staining with anti-Pax2 antibody, which labels the WD, MesM, and MesTs, shown in red (G and H) or white (I and J). Multiple stacked confocal images were reconstructed into one continuous image, where the borders of individual images are indicated by the dashed lines and the WDs (I and J) are pseudocolored in green for ease of identification. The arrows indicate the caudalmost MesM. The insets show enlarged images of the boxed regions. Scale bar, 1 mm. (K) Length between the rostral end of the WD and the point where the caudalmost MesM exists relative to the length of the WD (means ± SD; $n = 5$).

positioning of its precursor, the posterior IM, at E9.5. After E9.5, in *Ror2*$^{-/-}$ and *Wnt5a*$^{-/-}$ embryos, the MM differentiated from the posterior IM may fail to grow thoroughly in the metanephric region, resulting in mispositioning of the MM, while the caudally developing MesM may abnormally differentiate into the MesTs in close proximity to the metanephric region. Nevertheless, it is still possible that a secondary change in the organization of the metanephric field would occur due to gross alterations in posterior extension, since we have not explored in depth the formative period between E9.5 and E10.5. Thus, we also cannot rule out the possibility that the ectopic MesTs influence the normal development of the MM, although the mutant kidneys with ectopic MesTs did not necessarily show UB phenotypes.

In summary, we show here that noncanonical Wnt5a-Ror2 signaling plays an important role in regulating proper formation of the MM, at least partly by mediating cell proliferation. As suggested by our present study and other studies (37), the MM progressively migrates or accumulates from the anterior ventral side of the caudal WD to the region of the future MM (the dorsal side of the caudal end of the WD). Thus, our results suggest that, in addition to cell proliferation, mesenchymal cell migration is impaired in *Ror2*$^{-/-}$ and *Wnt5a*$^{-/-}$ kidneys, resulting in more anterior and diffuse distribution of a *Gdnf*-expressing MM. Aberrant formation of the MM in the mutant kidneys gives rise to inappropriate interaction between the MM and WD due to abnormal positioning of the MM, resulting in inappropriate GDNF signaling at the WD, leading to ectopic budding. The ectopic UBs in turn maintain ectopic *Gdnf* expression for their further outgrowth and branching morphogenesis. However, *Wnt5a*$^{-/-}$ kidneys with more severe phenotypes fail to create proper interaction between the MM and WD or UB, resulting in loss of *Gdnf* expression and impaired outgrowth and branching of the UB. Further studies will be required to clarify the role of Wnt5a-Ror2 signaling in mesenchymal cell migration during ureteric budding. It is also important to examine *Ror1 Ror2*-double mutants to clarify the possible functional redundancy between Ror1 and Ror2 and to elucidate further the mechanisms by which Wnt5a-Ror signaling regulates kidney development.

ACKNOWLEDGMENTS

We thank G. Martin for the *Slit2* probe and T. Kume for the *Foxc1* probe. We also thank R. Onishi and X. Qi for technical assistance and M. Endo (Kobe University) for critical reading of the manuscript.

This work was supported by grants-in-aid for Scientific Research (B) (Y.M.), for Scientific Research on Innovative Areas (23112007 [Y.M.] and 25111717 [M.N.]), and for the Global Center of Excellence Program (Y.M) from the Ministry of Education, Culture, Sports, Science, and Technology, Japan; by grants from the Terumo Life Science Foundation (M.N.); and by the program of the Joint Usage/Research Center for Developmental Medicine, Institute of Molecular Embryology and Genetics, Kumamoto University (M.N.).

REFERENCES

1. **Oishi I, Suzuki H, Onishi N, Takada R, Kani S, Ohkawara B, Koshida I, Suzuki K, Yamada G, Schwabe GC, Mundlos S, Shibuya H, Takada S, Minami Y.** 2003. The receptor tyrosine kinase Ror2 is involved in non-canonical Wnt5a/JNK signalling pathway. Genes Cells **8:**645–654. http://dx.doi.org/10.1046/j.1365-2443.2003.00662.x.
2. **Mikels AJ, Nusse R.** 2006. Purified Wnt5a protein activates or inhibits beta-catenin-TCF signaling depending on receptor context. PLoS Biol. **4:**e115. http://dx.doi.org/10.1371/journal.pbio.0040115.
3. **Nishita M, Enomoto M, Yamagata K, Minami Y.** 2010. Cell/tissue-tropic functions of Wnt5a signaling in normal and cancer cells. Trends Cell Biol. **20:**346–354. http://dx.doi.org/10.1016/j.tcb.2010.03.001.
4. **Nishita M, Itsukushima S, Nomachi A, Endo M, Wang Z, Inaba D, Qiao S, Takada S, Kikuchi A, Minami Y.** 2010. Ror2/Frizzled complex mediates Wnt5a-induced AP-1 activation by regulating Dishevelled polymerization. Mol. Cell. Biol. **30:**3610–3619. http://dx.doi.org/10.1128/MCB.00177-10.
5. **Nishita M, Yoo SK, Nomachi A, Kani S, Sougawa N, Ohta Y, Takada S, Kikuchi A, Minami Y.** 2006. Filopodia formation mediated by receptor tyrosine kinase Ror2 is required for Wnt5a-induced cell migration. J. Cell Biol. **175:**555–562. http://dx.doi.org/10.1083/jcb.200607127.
6. **Schambony A, Wedlich D.** 2007. Wnt-5A/Ror2 regulate expression of XPAPC through an alternative noncanonical signaling pathway. Dev. Cell **12:**779–792. http://dx.doi.org/10.1016/j.devcel.2007.02.016.
7. **Nomachi A, Nishita M, Inaba D, Enomoto M, Hamasaki M, Minami Y.** 2008. Receptor tyrosine kinase Ror2 mediates Wnt5a-induced polarized cell migration by activating c-Jun N-terminal kinase via actin-binding protein Filamin A. J. Biol. Chem. **283:**27973–27981. http://dx.doi.org/10.1074/jbc.M802325200.
8. **He F, Xiong W, Yu X, Espinoza-Lewis R, Liu C, Gu S, Nishita M, Suzuki K, Yamada G, Minami Y, Chen Y.** 2008. Wnt5a regulates directional cell migration and cell proliferation via Ror2-mediated noncanonical pathway in mammalian palate development. Development **135:**3871–3879. http://dx.doi.org/10.1242/dev.025767.
9. **Laird DJ, Altshuler-Keylin S, Kissner MD, Zhou X, Anderson KV.** 2011. Ror2 enhances polarity and directional migration of primordial germ cells. PLoS Genet. **7:**e1002428. http://dx.doi.org/10.1371/journal.pgen.1002428.
10. **Gao B, Song H, Bishop K, Elliot G, Garrett L, English MA, Andre P, Robinson J, Sood R, Minami Y, Economides AN, Yang Y.** 2011. Wnt signaling gradients establish planar cell polarity by inducing Vangl2 phosphorylation through Ror2. Dev. Cell **20:**163–176. http://dx.doi.org/10.1016/j.devcel.2011.01.001.
11. **O'Connell MP, Fiori JL, Xu M, Carter AD, Frank BP, Camilli TC, French AD, Dissanayake SK, Indig FE, Bernier M, Taub DD, Hewitt SM, Weeraratna AT.** 2010. The orphan tyrosine kinase receptor, ROR2, mediates Wnt5A signaling in metastatic melanoma. Oncogene **29:**34–44. http://dx.doi.org/10.1038/onc.2009.305.
12. **Endo M, Doi R, Nishita M, Minami Y.** 2012. Ror family receptor tyrosine kinases regulate the maintenance of neural progenitor cells in the developing neocortex. J. Cell Sci. **125:**2017-2029. http://dx.doi.org/10.1242/jcs.097782.
13. **Al-Shawi R, Ashton SV, Underwood C, Simons JP.** 2001. Expression of the Ror1 and Ror2 receptor tyrosine kinase genes during mouse development. Dev. Genes Evol. **211:**161–171. http://dx.doi.org/10.1007/s004270100140.
14. **Matsuda T, Nomi M, Ikeya M, Kani S, Oishi I, Terashima T, Takada S, Minami Y.** 2001. Expression of the receptor tyrosine kinase genes, Ror1 and Ror2, during mouse development. Mech. Dev. **105:**153–156. http://dx.doi.org/10.1016/S0925-4773(01)00383-5.
15. **Yamaguchi TP, Bradley A, McMahon AP, Jones S.** 1999. A Wnt5a pathway underlies outgrowth of multiple structures in the vertebrate embryo. Development **126:**1211–1223.
16. **DeChiara TM, Kimble RB, Poueymirou WT, Rojas J, Masiakowski P, Valenzuela DM, Yancopoulos GD.** 2000. Ror2, encoding a receptor-like tyrosine kinase, is required for cartilage and growth plate development. Nat. Genet. **24:**271–274. http://dx.doi.org/10.1038/73488.
17. **Minami Y, Oishi I, Endo M, Nishita M.** 2010. Ror-family receptor tyrosine kinases in noncanonical Wnt signaling: Their implications in developmental morphogenesis and human diseases. Dev. Dyn. **239:**1–15. http://dx.doi.org/10.1002/dvdy.21991.
18. **Takeuchi S, Takeda K, Oishi I, Nomi M, Ikeya M, Itoh K, Tamura S, Ueda T, Hatta T, Otani H, Terashima T, Takada S, Yamamura H, Akira S, Minami Y.** 2000. Mouse Ror2 receptor tyrosine kinase is required for the heart development and limb formation. Genes Cells **5:**71–78. http://dx.doi.org/10.1046/j.1365-2443.2000.00300.x.
19. **Afzal AR, Rajab A, Fenske CD, Oldridge M, Elanko N, Ternes-Pereira E, Tuysuz B, Murday VA, Patton MA, Wilkie AO, Jeffery S.** 2000. Recessive Robinow syndrome, allelic to dominant brachydactyly type B, is caused by mutation of ROR2. Nat. Genet. **25:**419–422. http://dx.doi.org/10.1038/78107.
20. **van Bokhoven H, Celli J, Kayserili H, van Beusekom E, Balci S, Brussel W, Skovby F, Kerr B, Percin EF, Akarsu N, Brunner HG.** 2000. Muta-

tion of the gene encoding the ROR2 tyrosine kinase causes autosomal recessive Robinow syndrome. Nat. Genet. **25:**423–426. http://dx.doi.org/10.1038/78113.

21. **Soliman AT, Rajab A, Alsalmi I, Bedair SM.** 1998. Recessive Robinow syndrome: with emphasis on endocrine functions. Metabolism **47:**1337–1343. http://dx.doi.org/10.1016/S0026-0495(98)90301-8.
22. **Tufan F, Cefle K, Turkmen S, Turkmen A, Zorba U, Dursun M, Ozturk S, Palanduz S, Ecder T, Mundlos S, Horn D.** 2005. Clinical and molecular characterization of two adults with autosomal recessive Robinow syndrome. Am. J. Med. Genet. A **136:**185–189. http://dx.doi.org/10.1002/ajmg.a.30785.
23. **Saxen L.** 1987. Organogenesis of the kidney. Cambridge University Press, Cambridge, United Kingdom.
24. **Pope JC, IV, Brock JW, III, Adams MC, Stephens FD, Ichikawa I.** 1999. How they begin and how they end: classic and new theories for the development and deterioration of congenital anomalies of the kidney and urinary tract, CAKUT. J. Am. Soc. Nephrol. **10:**2018–2028.
25. **Song R, Yosypiv IV.** 2012. Development of the kidney medulla. Organogenesis **8:**10–17. http://dx.doi.org/10.4161/org.19308.
26. **Cacalano G, Farinas I, Wang LC, Hagler K, Forgie A, Moore M, Armanini M, Phillips H, Ryan AM, Reichardt LF, Hynes M, Davies A, Rosenthal A.** 1998. GFRalpha1 is an essential receptor component for GDNF in the developing nervous system and kidney. Neuron **21:**53–62. http://dx.doi.org/10.1016/S0896-6273(00)80514-0.
27. **Enomoto H, Araki T, Jackman A, Heuckeroth RO, Snider WD, Johnson EM, Jr, Milbrandt J.** 1998. GFR alpha1-deficient mice have deficits in the enteric nervous system and kidneys. Neuron **21:**317–324. http://dx.doi.org/10.1016/S0896-6273(00)80541-3.
28. **Moore MW, Klein RD, Farinas I, Sauer H, Armanini M, Phillips H, Reichardt LF, Ryan AM, Carver-Moore K, Rosenthal A.** 1996. Renal and neuronal abnormalities in mice lacking GDNF. Nature **382:**76–79. http://dx.doi.org/10.1038/382076a0.
29. **Pichel JG, Shen L, Sheng HZ, Granholm AC, Drago J, Grinberg A, Lee EJ, Huang SP, Saarma M, Hoffer BJ, Sariola H, Westphal H.** 1996. Defects in enteric innervation and kidney development in mice lacking GDNF. Nature **382:**73–76. http://dx.doi.org/10.1038/382073a0.
30. **Sanchez MP, Silos-Santiago I, Frisen J, He B, Lira SA, Barbacid M.** 1996. Renal agenesis and the absence of enteric neurons in mice lacking GDNF. Nature **382:**70–73. http://dx.doi.org/10.1038/382070a0.
31. **Schuchardt A, D'Agati V, Larsson-Blomberg L, Costantini F, Pachnis V.** 1994. Defects in the kidney and enteric nervous system of mice lacking the tyrosine kinase receptor Ret. Nature **367:**380–383. http://dx.doi.org/10.1038/367380a0.
32. **Grieshammer U, Le M, Plump AS, Wang F, Tessier-Lavigne M, Martin GR.** 2004. SLIT2-mediated ROBO2 signaling restricts kidney induction to a single site. Dev. Cell **6:**709–717. http://dx.doi.org/10.1016/S1534-5807(04)00108-X.
33. **Kume T, Deng K, Hogan BL.** 2000. Murine forkhead/winged helix genes Foxc1 (Mf1) and Foxc2 (Mfh1) are required for the early organogenesis of the kidney and urinary tract. Development **127:**1387–1395.
34. **Basson MA, Akbulut S, Watson-Johnson J, Simon R, Carroll TJ, Shakya R, Gross I, Martin GR, Lufkin T, McMahon AP, Wilson PD, Costantini FD, Mason IJ, Licht JD.** 2005. Sprouty1 is a critical regulator of GDNF/RET-mediated kidney induction. Dev. Cell **8:**229–239. http://dx.doi.org/10.1016/j.devcel.2004.12.004.
35. **Srinivas S, Goldberg MR, Watanabe T, D'Agati V, al-Awqati Q, Costantini F.** 1999. Expression of green fluorescent protein in the ureteric bud of transgenic mice: a new tool for the analysis of ureteric bud morphogenesis. Dev. Genet. **24:**241–251.
36. **Kani S, Oishi I, Yamamoto H, Yoda A, Suzuki H, Nomachi A, Iozumi K, Nishita M, Kikuchi A, Takumi T, Minami Y.** 2004. The receptor tyrosine kinase Ror2 associates with and is activated by casein kinase Iepsilon. J. Biol. Chem. **279:**50102–50109. http://dx.doi.org/10.1074/jbc.M409039200.
37. **Hoshi M, Batourina E, Mendelsohn C, Jain S.** 2012. Novel mechanisms of early upper and lower urinary tract patterning regulated by RetY1015 docking tyrosine in mice. Development **139:**2405–2415. http://dx.doi.org/10.1242/dev.078667.
38. **Yamada M, Udagawa J, Matsumoto A, Hashimoto R, Hatta T, Nishita M, Minami Y, Otani H.** 2010. Ror2 is required for midgut elongation during mouse development. Dev. Dyn. **239:**941–953. http://dx.doi.org/10.1002/dvdy.22212.
39. **Nishinakamura R, Matsumoto Y, Nakao K, Nakamura K, Sato A, Copeland NG, Gilbert DJ, Jenkins NA, Scully S, Lacey DL, Katsuki M, Asashima M, Yokota T.** 2001. Murine homolog of SALL1 is essential for ureteric bud invasion in kidney development. Development **128:**3105–3115.
40. **Ren D, Minami Y, Nishita M.** 2011. Critical role of Wnt5a-Ror2 signaling in motility and invasiveness of carcinoma cells following Snail-mediated epithelial-mesenchymal transition. Genes Cells **16:**304–315. http://dx.doi.org/10.1111/j.1365-2443.2011.01487.x.
41. **Jahan E, Matsumoto A, Udagawa J, Rafiq AM, Hashimoto R, Rahman OI, Habib H, Sekine J, Otani H.** 2010. Effects of restriction of fetal jaw movement on prenatal development of the temporalis muscle. Arch. Oral Biol. **55:**919–927. http://dx.doi.org/10.1016/j.archoralbio.2010.07.010.
42. **Georgas KM, Chiu HS, Lesieur E, Rumballe BA, Little MH.** 2011. Expression of metanephric nephron-patterning genes in differentiating mesonephric tubules. Dev. Dyn. **240:**1600–1612. http://dx.doi.org/10.1002/dvdy.22640.
43. **Mackie GG, Stephens FD.** 1975. Duplex kidneys: a correlation of renal dysplasia with position of the ureteral orifice. J. Urol. **114:**274–280.
44. **Batourina E, Choi C, Paragas N, Bello N, Hensle T, Costantini FD, Schuchardt A, Bacallao RL, Mendelsohn CL.** 2002. Distal ureter morphogenesis depends on epithelial cell remodeling mediated by vitamin A and Ret. Nat. Genet. **32:**109–115. http://dx.doi.org/10.1038/ng952.
45. **Kaku Y, Ohmori T, Kudo K, Fujimura S, Suzuki K, Evans SM, Kawakami Y, Nishinakamura R.** 2013. Islet1 deletion causes kidney agenesis and hydroureter resembling CAKUT. J. Am. Soc. Nephrol. **24:**1242–1249. http://dx.doi.org/10.1681/ASN.2012050528.
46. **Gotoh H, Masuzaki H, Taguri H, Yoshimura S, Ishimaru T.** 1998. Effect of experimentally induced urethral obstruction and surgical decompression in utero on renal development and function in rabbits. Early Hum. Dev. **52:**111–123. http://dx.doi.org/10.1016/S0378-3782(98)00020-6.
47. **McVary KT, Maizels M.** 1989. Urinary obstruction reduces glomerulogenesis in the developing kidney: a model in the rabbit. J. Urol. **142:**646–651, 667–668.
48. **Temelcos C, Hutson JM.** 2004. Ontogeny of the VATER kidney in a rat model. Anat. Rec. A Discov. Mol. Cell. Evol. Biol. **278:**520–527. http://dx.doi.org/10.1002/ar.a.20030.
49. **Whitten SM, Wilcox DT.** 2001. Duplex systems. Prenat. Diagn. **21:**952–957. http://dx.doi.org/10.1002/pd.206.
50. **Fisher CE, Michael L, Barnett MW, Davies JA.** 2001. Erk MAP kinase regulates branching morphogenesis in the developing mouse kidney. Development **128:**4329–4338.
51. **Watanabe T, Costantini F.** 2004. Real-time analysis of ureteric bud branching morphogenesis in vitro. Dev. Biol. **271:**98–108. http://dx.doi.org/10.1016/j.ydbio.2004.03.025.
52. **Majumdar A, Vainio S, Kispert A, McMahon J, McMahon AP.** 2003. Wnt11 and Ret/Gdnf pathways cooperate in regulating ureteric branching during metanephric kidney development. Development **130:**3175–3185. http://dx.doi.org/10.1242/dev.00520.
53. **Mugford JW, Sipila P, Kobayashi A, Behringer RR, McMahon AP.** 2008. Hoxd11 specifies a program of metanephric kidney development within the intermediate mesoderm of the mouse embryo. Dev. Biol. **319:**396–405. http://dx.doi.org/10.1016/j.ydbio.2008.03.044.
54. **Carroll TJ, Park JS, Hayashi S, Majumdar A, McMahon AP.** 2005. Wnt9b plays a central role in the regulation of mesenchymal to epithelial transitions underlying organogenesis of the mammalian urogenital system. Dev. Cell **9:**283–292. http://dx.doi.org/10.1016/j.devcel.2005.05.016.
55. **Taguchi A, Kaku Y, Ohmori T, Sharmin S, Ogawa M, Sasaki H, Nishinakamura R.** 2014. Redefining the in vivo origin of metanephric nephron progenitors enables generation of complex kidney structures from pluripotent stem cells. Cell Stem Cell **14:**53–67. http://dx.doi.org/10.1016/j.stem.2013.11.010.
56. **Wellik DM, Hawkes PJ, Capecchi MR.** 2002. Hox11 paralogous genes are essential for metanephric kidney induction. Genes Dev. **16:**1423–1432. http://dx.doi.org/10.1101/gad.993302.